WNT/RYK signaling restricts goblet cell differentiation during lung development and repair

Hyun-Taek Kim[a,1], Wenguang Yin[a], Yuko Nakamichi[b], Paolo Panza[a], Beate Grohmann[a], Carmen Buettner[a], Stefan Guenther[c], Clemens Ruppert[d], Yasuhiro Kobayashi[b], Andreas Guenther[d], and Didier Y. R. Stainier[a,1]

[a]Department of Developmental Genetics, Max Planck Institute for Heart and Lung Research, 61231 Bad Nauheim, Germany; [b]Institute for Oral Science, Matsumoto Dental University, 399-0781 Shiojiri, Japan; [c]Bioinformatics and Deep Sequencing Platform, Max Planck Institute for Heart and Lung Research, 61231 Bad Nauheim, Germany; and [d]Biobank, University of Giessen & Marburg Lung Center, 35392 Giessen, Germany

Edited by Edward E. Morrisey, University of Pennsylvania, Philadelphia, PA, and accepted by Editorial Board Member Roeland Nusse November 1, 2019 (received for review June 27, 2019)

Goblet cell metaplasia and mucus hypersecretion are observed in many pulmonary diseases, including asthma, chronic obstructive pulmonary disease (COPD), and cystic fibrosis. However, the regulation of goblet cell differentiation remains unclear. Here, we identify a regulator of this process in an *N*-ethyl-*N*-nitrosourea (ENU) screen for modulators of postnatal lung development; *Ryk* mutant mice exhibit lung inflammation, goblet cell hyperplasia, and mucus hypersecretion. RYK functions as a WNT coreceptor, and, in the developing lung, we observed high RYK expression in airway epithelial cells and moderate expression in mesenchymal cells as well as in alveolar epithelial cells. From transcriptomic analyses and follow-up studies, we found decreased WNT/β-catenin signaling activity in the mutant lung epithelium. Epithelial-specific *Ryk* deletion causes goblet cell hyperplasia and mucus hypersecretion but not inflammation, while club cell-specific *Ryk* deletion in adult stages leads to goblet cell hyperplasia and mucus hypersecretion during regeneration. We also found that the airway epithelium of COPD patients often displays goblet cell metaplastic foci, as well as reduced RYK expression. Altogether, our findings reveal that RYK plays important roles in maintaining the balance between airway epithelial cell populations during development and repair, and that defects in RYK expression or function may contribute to the pathogenesis of human lung diseases.

RYK | WNT/β-catenin signaling | goblet cell hyperplasia | COPD | lung

Goblet cell metaplasia and mucus hypersecretion are features of lung diseases, including asthma, chronic obstructive pulmonary disease (COPD), and pulmonary fibrosis (1, 2). In chronic airway diseases, mucus hypersecretion and mucus plugging leads to airway obstruction and contributes significantly to morbidity and mortality (3). Goblet cells differentiate from club cells, and this process is controlled by a number of extrinsic and intrinsic factors, including EGFR (epidermal growth factor receptor), NOTCH, and SPDEF (Sam-pointed domain Ets-like factor) (4, 5). Additional studies have addressed which inflammatory signals and growth factors drive goblet cell metaplasia and mucus hypersecretion (3, 6, 7). However, the underlying molecular mechanisms are not completely understood.

WNT signaling plays critical roles during development and homeostasis, including during cell proliferation and differentiation, as well as during tissue morphogenesis (8–10). Many WNT ligands, receptors, and intracellular effectors, including transcription factors, exhibit highly specific expression in developing lungs (10, 11). Genetic studies have uncovered crucial roles for WNT signaling in lung morphogenesis and homeostasis. For example, in mouse, loss of *Wnt-2* (12) or *Wnt-4* (13) leads to lung hypoplasia, and loss of *Wnt-5a* leads to hypoplastic tracheas and abnormal distal lung structure (14). Additionally, loss of β-catenin leads to trachea and lung agenesis (15), while its stabilization in epithelial cells results in trachea formation defects and dilation of distal airways (16). Club cell-specific β-catenin activation at later stages causes goblet cell metaplasia, pulmonary tumor development, and airspace enlargement (17). However, the molecular mechanisms by which WNT signaling regulates airway epithelial differentiation during postnatal lung development and regeneration remain poorly understood.

Related to tyrosine kinase (RYK), a WNT coreceptor, belongs to the atypical receptor tyrosine kinase family (18, 19). The functions of RYK have been studied in several model organisms, including *Drosophila* (20), zebrafish (21), *Xenopus* (22), and mouse (23). RYK binds to WNTs via its WIF domain and modulates both β-catenin–dependent (canonical) and β-catenin–independent (noncanonical) signaling pathways to regulate cell polarity, cell migration, cell fate determination, and skeletal development, as well as neurogenesis and axon guidance (24, 25). In mouse, *Ryk* knockout leads to growth retardation, defects in craniofacial and skeletal development, and postnatal lethality (23). In vitro studies have shown that RYK binds to WNTs, Frizzled (FZD) 8, and Dishevelled (DVL) proteins to activate β-catenin/TCF-dependent transcription (26, 27). In addition, *Ryk* interacts genetically with *Van Gogh-like 2* (*Vangl2*) (28), a core planar cell polarity (PCP) signaling component, and $Vangl2^{-/-};Ryk^{-/-}$ mice exhibit classical PCP phenotypes including defects in neural tube closure, in the elongation of the anteroposterior body axis,

Significance

Goblet cell metaplasia and mucus hypersecretion are observed in many pulmonary diseases. However, the regulation of goblet cell differentiation remains unclear. We identified an ENU-induced mutation in the mouse *Ryk* gene which causes goblet cell hyperplasia in the lung. From transcriptomic analyses and follow-up studies, we found decreased WNT/β-catenin signaling activity in the airway epithelium of mutant lungs. Epithelial-specific *Ryk* deletion causes goblet cell hyperplasia and mucus hypersecretion during lung development and repair. We also found that the airway epithelium of COPD patients often displays goblet cell metaplastic foci, as well as reduced RYK expression, suggesting a conserved role for RYK in the regulation of goblet cell fate in both development and disease.

Author contributions: H.-T.K. and D.Y.R.S. designed research; H.-T.K., W.Y., Y.N., P.P., B.G., C.B., S.G., and Y.K. performed research; Y.N., C.R., Y.K., and A.G. contributed new reagents/analytic tools; H.-T.K., W.Y., Y.N., S.G., and D.Y.R.S. analyzed data; and H.-T.K., P.P., and D.Y.R.S. wrote the paper.

The authors declare no competing interest.

This article is a PNAS Direct Submission. E.E.M. is a guest editor invited by the Editorial Board.

Data deposition: The RNA-Seq data reported in this paper have been deposited in the Gene Expression Omnibus (GEO) database, https://www.ncbi.nlm.nih.gov/geo/query/acc.cgi?acc=GSE131946 (accession no. GSE131946).

[1]To whom correspondence may be addressed. Email: Hyun-Taek.Kim@mpi-bn.mpg.de or didier.stainier@mpi-bn.mpg.de.

This article contains supporting information online at https://www.pnas.org/lookup/suppl/doi:10.1073/pnas.1911071116/-/DCSupplemental.

First published November 27, 2019.

and in craniofacial morphogenesis (28, 29). Recent studies reveal that RYK participates in mammary epithelial growth and branching morphogenesis (30) as well as in cardiac development (31). However, the potential role of RYK in lung development and homeostasis has not been studied.

The conducting airways of the lung are lined by a simple columnar epithelium containing multiciliated cells, basal cells, neuroendocrine cells, and secretory cells (32). The mucus-producing goblet cells are specialized secretory cells found throughout the mucosal epithelia in the gastrointestinal tract, airway, and ocular surface, and they are required for lubrication and barrier function against external pathogens and debris (33). Several growth factors, inflammatory cytokines, and transcription factors have been implicated in goblet cell differentiation and mucin production in the airway (6, 7). For instance, overexpression of Notch1 intracellular domain in airway epithelial cells leads to increased airway mucous cells and fewer ciliated cells (34). Airway epithelial cell-specific *Foxp1/4* knockout mice exhibit ectopic activation of the goblet cell lineage program (35). SPDEF regulates a transcriptional network required for airway goblet cell differentiation, and its overexpression is sufficient to cause goblet cell metaplasia in lung (36, 37). Overexpression of *Foxa3* in club cells causes goblet cell metaplasia and pulmonary inflammation (38). However, the roles of WNT/RYK signaling in airway goblet cell differentiation remain poorly understood.

In the present study, we reveal a role for RYK in the differentiation of airway epithelial cells during lung development and regeneration. Notably, we find that *Ryk* deficiency leads to decreased activity of WNT/β-catenin signaling in the lung epithelium as well as increased expression of genes associated with goblet cell hyperplasia in the lung epithelium in vitro and in vivo. Consistent with *Ryk* expression, epithelial cell-specific *Ryk* deletion leads to goblet cell hyperplasia and mucus hypersecretion during postnatal lung development and epithelial cell regeneration. Our results bring mechanistic insight into the regulation of lung epithelial cell differentiation, and how this program goes awry in disease, leading to goblet cell hyperplasia and mucus hypersecretion.

Results

An *N*-ethyl-*N*-nitrosourea Mutant Displays Growth Retardation and Goblet Cell Hyperplasia. To identify regulators of early postnatal lung development in mouse, we performed *N*-ethyl-*N*-nitrosourea (ENU) mutagenesis (39, 40). From screening the F3 progeny of 170 G1 mice, we identified 10 families displaying recessive lung inflammation phenotypes. In one of these families, mutant pups exhibited growth retardation and low body weight (Fig. 1 *A* and *B*) around postnatal day 1 (P1) and subsequently died around P14 (Fig. 1*C*). The mutant lungs were hypoplastic (Fig. 1*D*) and characterized by severe infiltration of inflammatory cells into airway lumens and alveolar spaces, as well as alveolar simplification (Fig. 1 *E* and *F*). Since viscous material was observed in airway lumens and alveolar spaces, we tested whether secretory cells, especially goblet cells, were affected in the mutant animals. Alcian blue staining and immunostainings revealed a massively

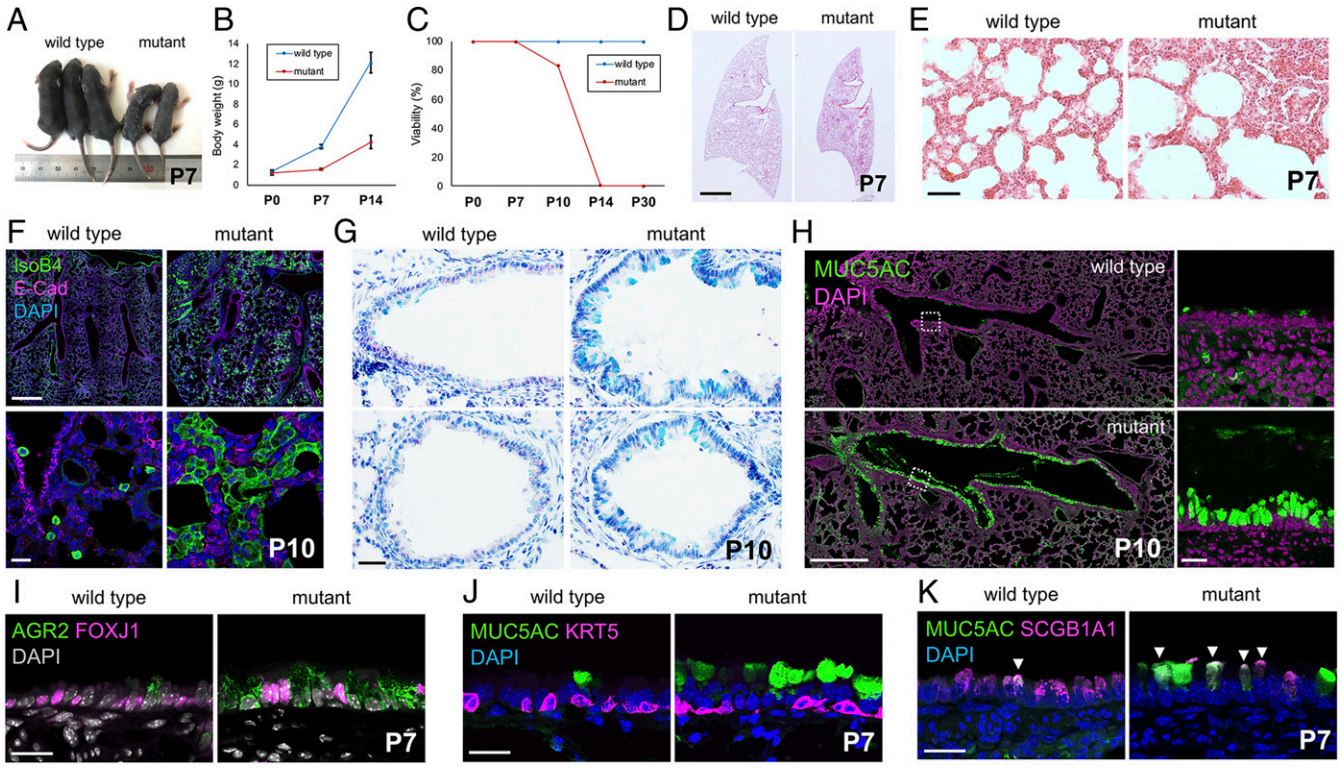

Fig. 1. An ENU-induced mutant exhibits goblet cell hyperplasia in the lung. (*A*) General appearance of P7 wild-type ($n = 30$) and mutant ($n = 20$) mice. (*B*) Body weight progression at postnatal stages of wild-type ($n = 12$) and mutant ($n = 12$) mice. (*C*) Survival rate of wild-type and mutant mice during postnatal development. Genotyping of 48 pups at P0, 52 pups at P7, 36 pups at P10, 25 pups at P14, and 20 pups at P30. (*D*) Hematoxylin and Eosin (H&E) staining of P7 wild-type ($n = 20$) and mutant ($n = 12$) lung sections. (*E*) High magnification of H&E-stained P7 wild-type ($n = 20$) and mutant ($n = 12$) lung sections. (*F*) Immunostaining for E-cadherin (E-Cad) and Isolectin B4 (IsoB4) in P10 wild-type ($n = 12$) and mutant ($n = 10$) lung sections. (*G*) Alcian blue/nuclear fast red staining in P10 wild-type ($n = 12$) and mutant ($n = 10$) lung sections. (*H*) Immunostaining for MUC5AC in P10 wild-type ($n = 12$) and mutant ($n = 10$) lung sections. A high-magnification image of the area in the dashed boxes is shown on the *Right*. (*I*) Immunostaining for AGR2 and FOXJ1 in P7 wild-type ($n = 12$) and mutant ($n = 10$) lung sections. (*J*) Immunostaining for MUC5AC and KRT5 in P7 wild-type ($n = 12$) and mutant ($n = 10$) lung sections. (*K*) Immunostaining for MUC5AC and SCGB1A1 in P7 wild-type ($n = 12$) and mutant ($n = 10$) lung sections. Arrowheads point to MUC5AC/SCGB1A1 double-positive/coexpressing cells. Error bars are means ± SEM. (Scale bars: *D*, 2 mm; *E*, 50 μm; *F* [*Top*] and *H* [*Left*], 500 μm; *F* [*Bottom*], *G*, *H* [*Right*], and *I*–*K*, 20 μm.)

increased number of mucus-containing secretory cells in the airway epithelium of mutant bronchi and bronchioles at P10 (Fig. 1*G*). While MUC5AC-positive goblet cells are rarely detected in the airway epithelium of wild-type animals at P10, the number of goblet cells was dramatically increased in mutant airway epithelium (Fig. 1*H*). In mutant lungs, goblet cells were found mainly along the distal tracheal tube and intrapulmonary conducting airway, extending from the primary bronchi to the bronchioles. Since goblet cells differentiate after birth (32), we determined the stage at which an increased goblet cell number was first observed in the mutants. Wheat germ agglutinin (WGA) lectin-positive mucin secreting cells (41) were increased in number at around P4 in mutant lungs (*SI Appendix*, Fig. S1*A*), correlating with the first wave of goblet cell differentiation (32).

In order to investigate the origin of the supernumerary goblet cells in the mutant airway epithelium, we first examined cellular proliferation and apoptosis in P7 wild-type and mutant lungs. Apoptotic cell death in the mutant airway epithelium was not significantly altered compared to wild type, even though it was increased in the mutant mesenchyme (*SI Appendix*, Fig. S1*B*). In contrast, cellular proliferation was significantly increased in the airway epithelium of mutant lungs (*SI Appendix*, Fig. S1*C*). Additionally, while the proliferation of basal (*SI Appendix*, Fig. S1*D*), ciliated (*SI Appendix*, Fig. S1*E*), and goblet cells (*SI Appendix*, Fig. S1*F*) was unaltered in mutant lungs, the number of proliferating club cells was significantly increased in mutant lungs compared to wild type (*SI Appendix*, Fig. S1 *G* and *H*). Next, we performed immunostaining for goblet cell markers (AGR2 and MUC5AC) in parallel with several airway epithelial cell markers, including FOXJ1 for ciliated cells, KRT5 for basal cells, and SCGB1A1 for club cells. In the mutant airway epithelium, markers of ciliated (Fig. 1*I*) and basal cells (Fig. 1*J*) did not overlap with goblet cell markers. Instead, many more goblet cells expressed club cell markers in mutants compared to wild type (Fig. 1*H*), suggesting that, in the mutant animals as in wild type, goblet cells derive from club cells.

A Stop-Loss Mutation in *Ryk* Is the Causal Variant in the Mutant. To identify the mutation causing the described phenotypes, we carried out whole-exome sequencing comparing wild-type and mutant genomes and found a stop-loss (SL) mutation (c.A1776G;p.X595W) in the *receptor-like tyrosine kinase* (*Ryk*) gene, which results in a 45-amino acid extension of the carboxy (C) terminus (*SI Appendix*, Fig. S2 *A* and *D*). The mutant allele could be distinguished by high-resolution melt analysis and Sanger sequencing (*SI Appendix*, Fig. S2 *B* and *C*). Since the C-terminal PDZ-binding motif in RYK acts as a ligand for DVL (26), we tested whether mutant RYK could physically interact with DVL1 by immunoprecipitating the RYK protein complex in HEK293T cells. While wild-type RYK stably interacts with DVL1, mutant RYK showed impaired binding to DVL1 (*SI Appendix*, Fig. S2*E*). This result indicates that the C-terminal RYK protein extension introduced by the SL mutation prevents the physical interaction between RYK and the PDZ domain of DVL1. To quantify the expression levels of *Ryk* messenger RNA (mRNA) and protein in mutant lungs, we performed RT-qPCR, Western blotting, and immunostaining. Expression of *Ryk* mRNA and protein was significantly decreased in $Ryk^{X595W/X595W}$ (hereafter $Ryk^{SL/SL}$) lungs compared with $Ryk^{+/+}$ and $Ryk^{X595W/+}$ (hereafter $Ryk^{SL/+}$) lungs (*SI Appendix*, Fig. S2 *F* and *G*). In addition, while RYK was strongly detected on the cell surface membranes of the airway epithelium in P4 $Ryk^{+/+}$ mice, it was weakly detected in $Ryk^{SL/SL}$ siblings (*SI Appendix*, Fig. S2*H*). These data suggest that the SL mutation in *Ryk* may induce mRNA decay and/or prevent the cell surface localization of the mutant protein.

Next, we performed complementation tests between the ENU-induced *Ryk* mutant and an *Ryk* null allele. To generate an *Ryk* null mouse, we inserted loxP sites upstream of exon 2 and downstream of exon 6 in the *Ryk* locus, encompassing a portion of the extracellular and transmembrane domain coding region (*SI Appendix*, Fig. S3 *A*–*C*), and then crossed the floxed allele with *CMV-Cre* mice. RYK protein expression was not detected in *CMV-Cre;*$Ryk^{fl/fl}$ (hereafter $Ryk^{-/-}$) lungs compared to wild-type littermates (*SI Appendix*, Fig. S3*D*). Transheterozygous mice, obtained by crossing $Ryk^{SL/+}$ with $Ryk^{+/-}$ mice, exhibited growth retardation and a lung phenotype identical to the *Ryk* global (23) and ENU-induced mutants, indicating that the loss of *Ryk* function is responsible for the observed lung phenotypes (*SI Appendix*, Fig. S3 *E*–*G*).

To determine the expression pattern of *Ryk* in developing lungs, we carried out in situ hybridization and immunostainings. At early embryonic stages, *Ryk* transcripts were detected in the airway epithelial tube (*SI Appendix*, Fig. S4*A*). At late gestation and early postnatal stages, *Ryk* was strongly expressed in airway epithelial cells and moderately expressed in blood vessels and in mesenchymal tissues (*SI Appendix*, Fig. S4*B*). RYK was similarly detected in airway epithelial cells at E12.5 (*SI Appendix*, Fig. S4*C*). At E18.5, RYK was detected in airway epithelium as well as in alveolar epithelial cells, but not in endothelial cells (*SI Appendix*, Fig. S4 *D* and *E*). Within the airway epithelium, RYK was strongly detected in ciliated and club cells but only weakly detected in basal and goblet cells (*SI Appendix*, Fig. S4*F*). In adult lungs, RYK was also specifically expressed in airway and alveolar epithelial cells as well as in immune cells (*SI Appendix*, Fig. S4 *G* and *H*). Altogether, we observed that, in the lung, RYK is strongly expressed in airway epithelial cells and moderately expressed in alveolar epithelial and mesenchymal cells.

RYK Functions as a Positive Regulator of WNT/β-Catenin Signaling in the Lung Epithelium. In order to understand the molecular mechanisms of RYK function during lung development, we analyzed the transcriptome of $Ryk^{+/+}$ and $Ryk^{SL/SL}$ lungs at P1 (Dataset S1). Many of the genes down-regulated in $Ryk^{SL/SL}$ lungs, including *Wnt2*, *Wnt7a*, *Rspo2*, *Wisp*, and *Shisa*, are known to be involved in the WNT/β-catenin signaling pathway (Fig. 2 *A* and *B*). We used RT-qPCR to further test the expression of these genes and observed a significant down-regulation of *Mycn*, *Shisa2*, *Shisa3*, *Rspo2*, *Wif1*, *Wisp*, *Wnt2*, and *Wnt7a* mRNA levels in $Ryk^{SL/SL}$ lungs compared to wild type (Fig. 2*C*). We also found significantly up-regulated genes in $Ryk^{SL/SL}$ lungs, including *Muc5b*, *Il1r2*, and *Il6ra* (Fig. 2*D*). Among the down-regulated genes, *Mycn* is known as a downstream target of WNT/β-catenin signaling, and it is expressed in airway and alveolar epithelial cells (42, 43). We tested *Mycn* expression in the airway epithelium by in situ hybridization and Western blotting. While *Mycn* mRNA expression was strongly detected in the airway epithelium of P1 wild-type animals, its expression was dramatically reduced in $Ryk^{SL/SL}$ lungs (Fig. 2*E*). In addition, MYCN expression was also reduced in $Ryk^{SL/SL}$ lungs compared to wild-type littermates (Fig. 2*F*). These data indicate that WNT/β-catenin signaling is down-regulated in *Ryk*-deficient lungs.

As RYK is known to modulate both β-catenin–dependent and β-catenin–independent signaling (18, 19), we first examined whether RYK participates in WNT/β-catenin signaling, by crossing Ryk^{SL} mutant mice with the TOPGAL reporter line. While β-catenin–dependent transcription was active in the airway epithelium of wild-type lungs, it was dramatically decreased in $Ryk^{SL/SL}$ airway epithelium (Fig. 2*G*). Next, we used a second WNT/β-catenin reporter (TOPFLASH) and observed that, in HEK293 cells, WNT-3A and RYK led to increased WNT/β-catenin reporter activation compared to basal levels (Fig. 2*H*). When *Ryk*-transfected cells were treated with WNT-3A, luciferase activity was further increased (Fig. 2*H*). However, treatment with WNT-5A, a β-catenin–independent WNT ligand, did not induce reporter activation. Simultaneous treatment with WNT-5A and *Ryk* induced the reporter at the same level as

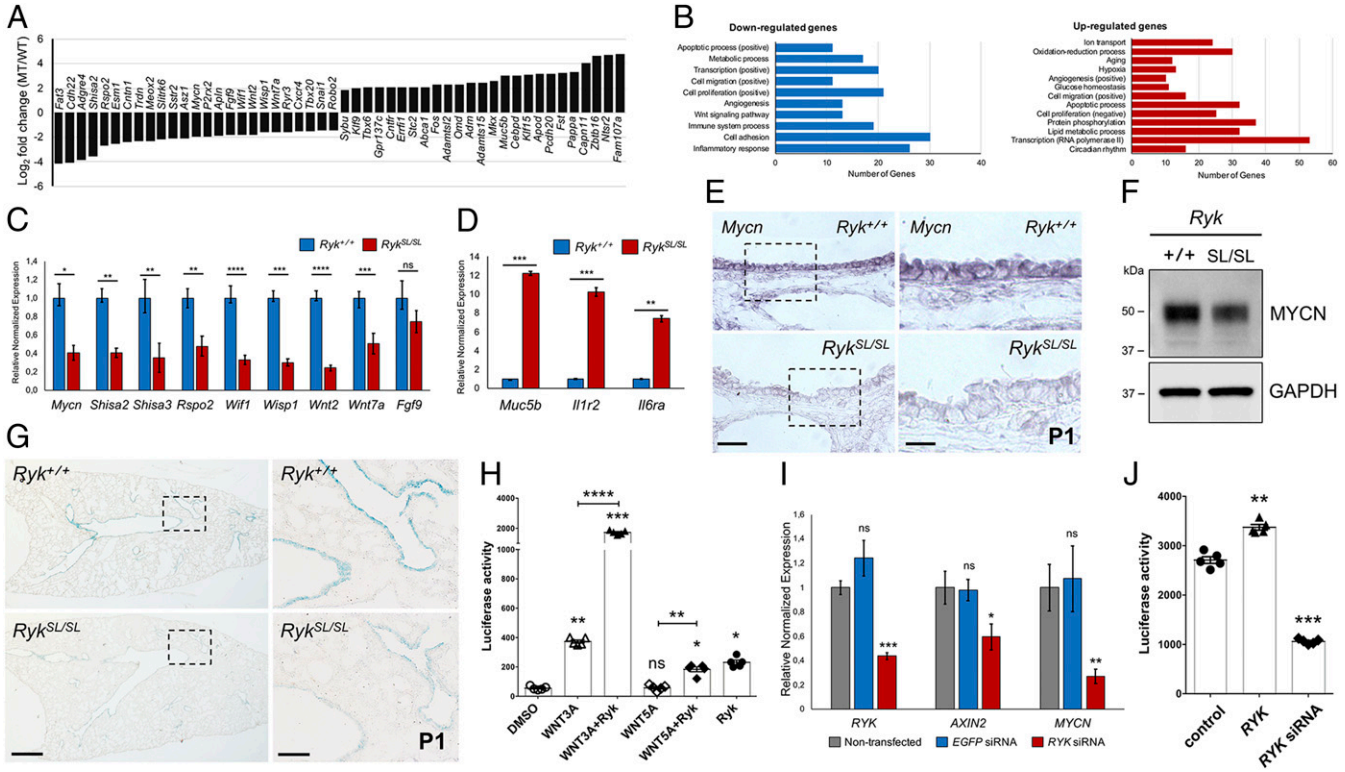

Fig. 2. RYK acts as a positive regulator of WNT/β-catenin signaling in the lung. (*A*) Differentially expressed genes (DEGs) between P1 $Ryk^{+/+}$ and $Ryk^{SL/SL}$ lungs from RNA-Seq analysis. Fold change (log_2) of DEGs (50 genes) in mutant compared to wild-type lungs. (*B*) Gene Ontology classification of DEGs between P1 $Ryk^{+/+}$ and $Ryk^{SL/SL}$ lungs. (*C*) The qPCR validation of down-regulated genes (WNT signaling-related genes and *Fgf9*) in P1 $Ryk^{+/+}$ and $Ryk^{SL/SL}$ lungs. (*D*) The qPCR validation of up-regulated genes (*Muc5b*, *Il1r2*, and *Il6ra*) in P1 $Ryk^{+/+}$ and $Ryk^{SL/SL}$ lungs. (*E*) *Mycn* expression in P1 $Ryk^{+/+}$ ($n = 6$) and $Ryk^{SL/SL}$ ($n = 4$) lung sections by in situ hybridization. A high-magnification image of the area in the dashed boxes is shown on the *Right*. (*F*) Representative Western blot (from 3 individual sets of lung lysates) for MYCN in P1 $Ryk^{+/+}$ and $Ryk^{SL/SL}$ lungs. GAPDH, glyceraldehyde-3-phosphate dehydrogenase. (*G*) X-gal staining of P1 $Ryk^{+/+}$;*TOPGAL* ($n = 6$) and $Ryk^{SL/SL}$;*TOPGAL* ($n = 6$) lung sections. A high-magnification image of the area in the dashed boxes is shown on the *Right*. (*H*) TOPFLASH-based WNT/β-catenin reporter assay upon stimulation with WNT3A or WNT5A or cotransfection of *Ryk*. (*I*) Expression levels of *RYK*, *AXIN2*, and *MYCN* in control small interfering RNA (siRNA) and *RYK* siRNA-treated HEK293T cells by RT-qPCR. (*J*) WNT/β-catenin reporter assay upon *Ryk* overexpression or *RYK* siRNA knockdown after transfection of the TOPFLASH reporter. Error bars are means ± SEM; ns, not significant; $^*P < 0.05$; $^{**}P < 0.01$; $^{***}P < 0.001$; $^{****}P < 0.0001$, 2-tailed Student's *t* test. Ct values are listed in *SI Appendix*, Table S2. (Scale bars: *E* [*Left*], 30 μm; *E* [*Right*], 10 μm; *G* [*Left*], 500 μm; *G* [*Right*], 100 μm.)

treatment with *Ryk* alone (Fig. 2*H*). Altogether, these data indicate that, in the airway epithelium, RYK is involved in the WNT/β-catenin signaling pathway. We next examined whether the loss of *RYK* leads to the down-regulation of WNT/β-catenin signaling activity. Expression of *AXIN2* and *MYCN*, targets of WNT/β-catenin signaling, was significantly decreased in *RYK* knockdown cells (Fig. 2*I*). While luciferase activity was significantly increased in cells overexpressing *RYK*, *RYK* knockdown led to decreased luciferase activity (Fig. 2*J*). As β-catenin–independent WNT signaling controls epithelial cell polarity and cell division orientation and RYK is known to also modulate β-catenin–independent signaling (8, 18, 19), we tested whether *Ryk* participates in these processes in the airway epithelium. Apicobasal polarity and mitotic spindle orientation of the airway epithelial cells did not appear to be altered in $Ryk^{SL/SL}$ lungs compared to wild type (*SI Appendix*, Fig. S5 *A* and *B*). In addition, since WNT/β-catenin signaling plays an important role in controlling fate determination between respiratory and digestive lineages (12, 15), we examined the expression of respiratory and digestive fate-related genes in embryonic $Ryk^{SL/SL}$ lungs. Most respiratory and foregut markers examined were down-regulated in E17.5 $Ryk^{SL/SL}$ lungs (*SI Appendix*, Fig. S5*C*), indicating that RYK does not participate in the selection between respiratory and foregut fates. To investigate whether the observed down-regulation of *Nkx2-1* was accompanied by the acquisition of hindgut/intestinal fates, as previously reported (44), we examined the expression of additional marker genes. The expression of hindgut/intestinal markers was unchanged (*SI Appendix*, Fig. S5*D*), indicating that epithelial cells in embryonic $Ryk^{SL/SL}$ lungs do not convert to a hindgut-like fate. Moreover, expression of NKX2-1 (respiratory epithelium) and SOX17 (digestive epithelium) was unaltered in $Ryk^{SL/SL}$ lungs compared to wild type (*SI Appendix*, Fig. S5 *E* and *F*). Overall, these results indicate that, in the airway epithelium, RYK acts as a positive effector in the WNT/β-catenin signaling pathway.

WNT/RYK Signaling Represses Genes Associated with Goblet Cell Hyperplasia. Among the genes up-regulated in our transcriptomic dataset, *MUC5B* is expressed by airway secretory cells, and it encodes a component of the mucous barrier protecting epithelial cells from the environment (45). To assess *Muc5b* expression in the airway epithelium, we performed in situ hybridization. *Muc5b* mRNA was detected in the airway epithelium of the trachea and distal airways of P0 wild-type animals (Fig. 3*A*). In $Ryk^{SL/SL}$ lungs, *Muc5b* expression was dramatically increased in proximal and distal airways (Fig. 3*A*). Whereas *Muc5b* mRNA was weakly expressed in club cells of wild-type lungs as previously reported (46), its expression was markedly increased in club cells but not in ciliated cells in P0 $Ryk^{SL/SL}$ lungs (Fig. 3*B*). MUC5B expression was also increased in P0 $Ryk^{SL/SL}$ lungs compared to wild-type and heterozygous littermates (Fig. 3*C*). At P4, while MUC5B was weakly expressed in wild-type airway epithelium (Fig. 3*D*), it was very highly expressed in proximal and distal airway epithelium of

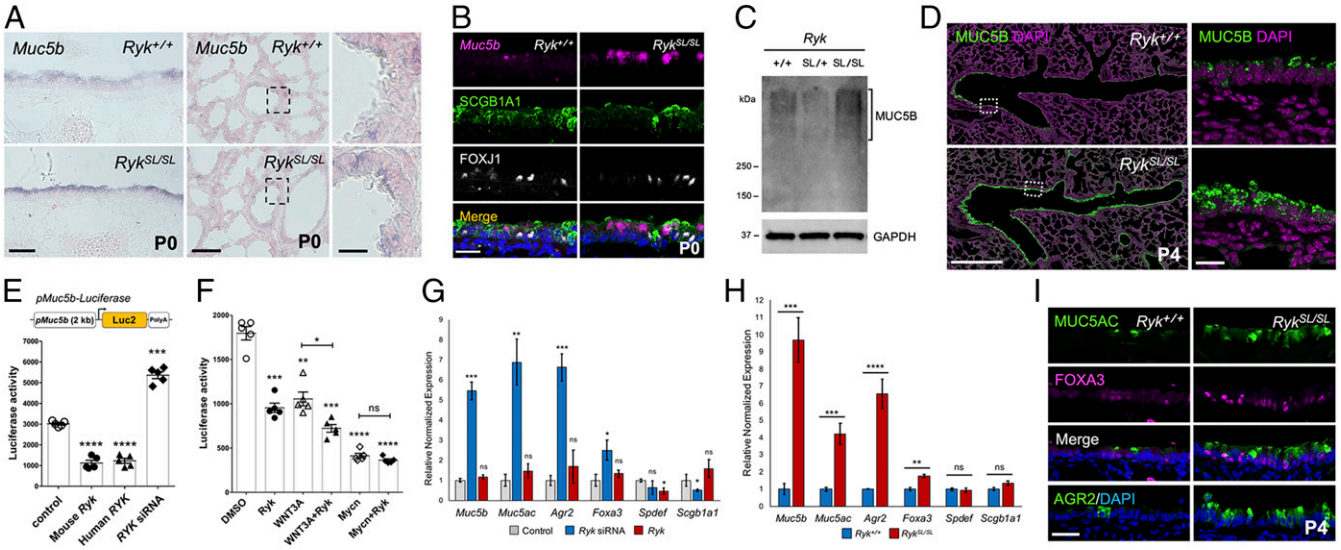

Fig. 3. WNT/RYK signaling inhibits goblet cell differentiation. (*A*) *Muc5b* expression in P0 $Ryk^{+/+}$ ($n = 6$) and $Ryk^{SL/SL}$ ($n = 4$) trachea (*Left*) and lung (*Middle* and *Right*) sections by in situ hybridization. A high-magnification image of the area in the dashed boxes (*Middle*) is shown on the *Right*. (*B*) Triple staining for *Muc5b* mRNA, SCGB1A1, and FOXJ1 in P0 $Ryk^{+/+}$ ($n = 6$) and $Ryk^{SL/SL}$ ($n = 4$) lung sections. (*C*) Representative Western blot (from 3 individual sets of lung lysates) for MUC5B in P4 $Ryk^{+/+}$, $Ryk^{SL/+}$, and $Ryk^{SL/SL}$ lungs. GAPDH, glyceraldehyde-3-phosphate dehydrogenase. (*D*) Immunostaining for MUC5B in P4 $Ryk^{+/+}$ ($n = 6$) and $Ryk^{SL/SL}$ ($n = 6$) lung sections. Dashed boxes refer to high-magnification images in the *Right* panels. (*E*) Luciferase assay measuring mouse *Muc5b* promoter activity in A549 cells upon transfection with mouse *Ryk*, human *RYK*, and *RYK* siRNA. (*F*) Luciferase assay measuring mouse *Muc5b* promoter activity in A549 cells upon stimulation with WNT3A and/or transfection with mouse *Ryk* as well as with transfection with *Mycn* without or with mouse *Ryk*. (*G*) Expression levels of lung epithelial cell markers in *Ryk* and *Ryk* siRNA-treated C22 club cells by RT-qPCR. (*H*) Expression levels of lung epithelial cell markers in P4 $Ryk^{+/+}$ and $Ryk^{SL/SL}$ lungs by RT-qPCR. (*I*) Immunostaining for MUC5AC, FOXA3, and AGR2 in P4 $Ryk^{+/+}$ ($n = 6$) and $Ryk^{SL/SL}$ ($n = 6$) lung sections. Error bars are means ± SEM; ns, not significant; $*P < 0.05$; $**P < 0.01$; $***P < 0.001$; $****P < 0.0001$, 2-tailed Student's *t* test. Ct values are listed in *SI Appendix*, Table S2. (Scale bars: *A* [*Left* and *Middle*] and *I*, 30 μm; *A* [*Right*], 10 μm; *B* and *D* [*Right*], 20 μm; *D* [*Left*], 500 μm.)

$Ryk^{SL/SL}$ lungs (Fig. 3*D*), indicating that *Ryk* negatively regulates *Muc5b* mRNA and protein expression in airway epithelial cells.

To test whether WNT/β-catenin signaling and RYK regulate *Muc5b* expression transcriptionally, we isolated a 2-kilobase mouse *Muc5b* promoter fragment and generated a *pMuc5b*-luciferase reporter construct (Fig. 3*E*). This reporter exhibited high basal activity in A549 human lung epithelial cells (Fig. 3*E*). However, while mouse and human *RYK* overexpression in A549 cells led to a reduction in *Muc5b* promoter activation, significantly increased luciferase activity was observed when *RYK* was knocked down (Fig. 3*E*). Moreover, WNT activation by WNT-3A inhibited the basal transcriptional activity from the *Muc5b* promoter (Fig. 3*F*). When WNT-3A was used in combination with *Ryk*, they acted synergistically to reduce luciferase activity (Fig. 3*F*). We also found that *Mycn* represses *Muc5b* promoter activity (Fig. 3*F*). However, when *Mycn* was cotransfected with *Ryk*, they showed no obvious synergistic effects on *Muc5b* promoter activity (Fig. 3*F*), indicating that WNT/RYK signaling represses *Muc5b* expression through MYCN in A549 lung epithelial cells.

Since *Ryk* deficiency leads to goblet cell hyperplasia in the lung, we next examined the expression of goblet cell hyperplasia-associated genes in vitro and in vivo. First, we used C22 cells, an immortalized mouse club cell line. When *Ryk* was knocked down in C22 cells, the expression of goblet cell hyperplasia-associated genes, *Muc5ac*, *Muc5b*, and *Agr2*, was dramatically increased, as was that of *Foxa3*, although to a lesser extent (Fig. 3*G*). The expression of *Spdef*, a regulator of goblet cell differentiation (36, 37), appeared to be unaltered in *Ryk* knockdown cells (Fig. 3*G*). However, the expression of these genes was not altered when we overexpressed *Ryk*, even though *Spdef* was down-regulated (Fig. 3*G*). The expression of *Scgb1a1*, a club cell marker, was also down-regulated in *Ryk* knockdown C22 cells (Fig. 3*G*). Next, we asked whether the hyperplasia signature was also present in $Ryk^{SL/SL}$ lungs at P4, the stage when goblet cell hyperplasia is first detectable. Similar to our *Ryk* knockdown results, the expression of *Muc5ac*, *Muc5b*, and *Agr2* was dramatically increased in P4 $Ryk^{SL/SL}$ lungs compared to wild-type littermates (Fig. 3*H*). The expression of *Foxa3* was also significantly increased (Fig. 3*H*). In contrast, *Spdef* and *Scgb1a1* expression was not changed in $Ryk^{SL/SL}$ lungs (Fig. 3*H*). MUC5AC, AGR2, and FOXA3 expression was also increased in the airway epithelium of P4 $Ryk^{SL/SL}$ lungs compared to wild-type littermates (Fig. 3*I*), indicating that RYK inhibits the expression of goblet cell hyperplasia-associated genes both in vitro and in vivo. Altogether, the up-regulation of goblet cell markers together with the down-regulation of club cell markers suggests that RYK inhibits club to goblet cell differentiation.

Epithelial-specific *Ryk* Deletion Leads to Goblet Cell Hyperplasia. To investigate its cell type-specific functions during mouse lung development, we deleted *Ryk* in a panepithelial manner using an *Shh-Cre* line and in club cells using a *CCSP-iCre* line. When we deleted *Ryk* in epithelial cells using *Shh-Cre* and Ryk^{flox} mice, RYK expression was dramatically decreased in the epithelium of *Shh-*Ryk^{cKO} lungs compared to wild-type littermates (Fig. 4*A*). Unlike *Ryk* KO (23) and $Ryk^{SL/SL}$ mice, *Shh-*Ryk^{cKO} mice showed no obvious growth retardation, lung hypoplasia, or lung inflammation (Fig. 4 *B–D* and *SI Appendix*, Fig. S6 *A* and *B*). Instead, *Shh-*Ryk^{cKO} mice exhibited a dramatically increased number of mucus-secreting cells in the airway epithelium as well as mucus hypersecretion into the airway lumen (Fig. 4*E*). In addition, the number of MUC5AC-positive goblet cells was massively increased in the bronchi and bronchioles of *Shh-*Ryk^{cKO} lungs compared to wild-type littermates (Fig. 4*F*). However, *Shh-*Ryk^{cKO} mice exhibited no obvious defects in the differentiation of alveolar epithelial cells (*SI Appendix*, Fig. S6*C*). Similar to what we observed in $Ryk^{SL/SL}$ mice, the number of MUC5B-positive cells and MUC5B expression were greatly increased in *Shh-*Ryk^{cKO} lungs compared to wild-type littermates (*SI Appendix*, Fig. S6 *D* and *E*). Whereas the number of ciliated cells did not appear to be altered

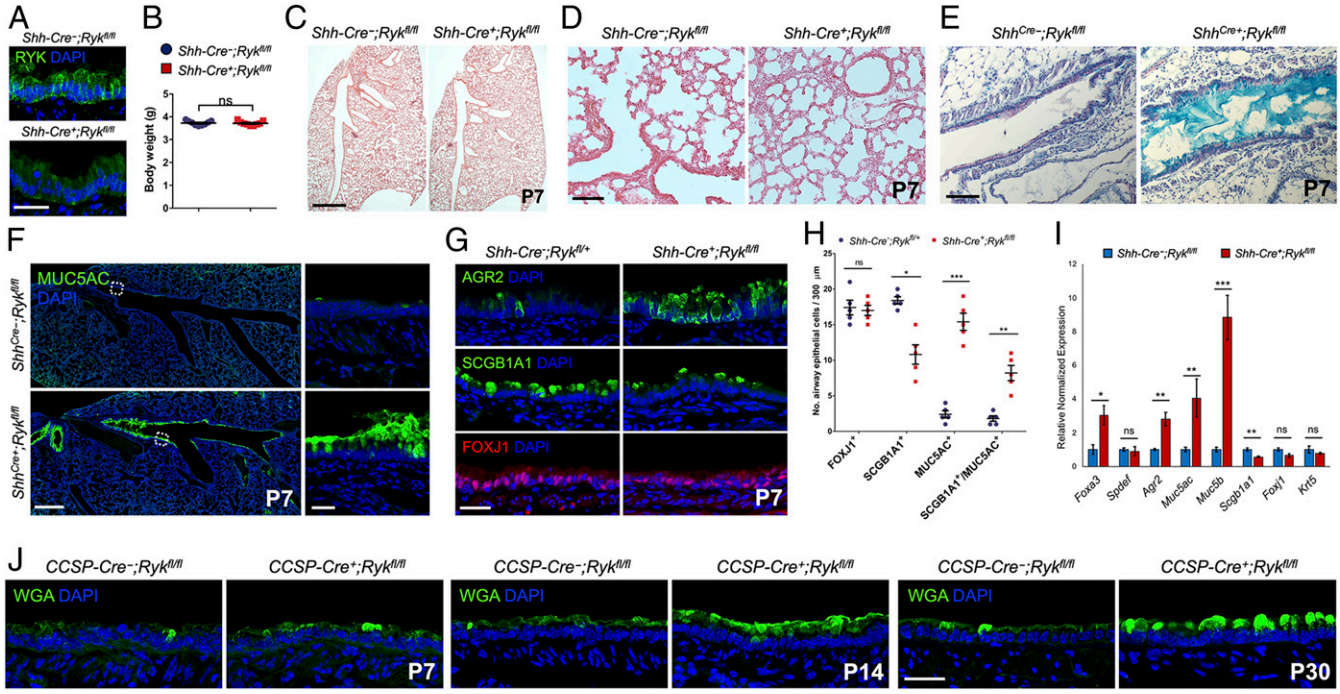

Fig. 4. Epithelial-specific *Ryk* deletion leads to goblet cell hyperplasia. (*A*) Immunostaining for RYK in P7 wild-type ($n = 12$) and *Shh-Ryk*^{cKO} ($n = 10$) lung sections. (*B*) Body weight of P7 wild-type ($n = 12$) and *Shh-Ryk*^{cKO} ($n = 10$) mice. (*C*) H&E staining of P7 wild-type ($n = 12$) and *Shh-Ryk*^{cKO} ($n = 10$) lung sections. (*D*) High magnification of H&E-stained P7 wild-type ($n = 12$) and *Shh-Ryk*^{cKO} ($n = 10$) lung sections. (*E*) Alcian blue staining for mucus-secreting goblet cells in P7 wild-type ($n = 12$) and *Shh-Ryk*^{cKO} ($n = 10$) lung sections. (*F*) Immunostaining for MUC5AC in P7 wild-type ($n = 12$) and *Shh-Ryk*^{cKO} ($n = 10$) lung sections. A high-magnification image of the area in the dashed boxes is shown on the *Right*. (*G*) Immunostaining for airway epithelial cell markers in P7 wild-type ($n = 12$) and *Shh-Ryk*^{cKO} ($n = 10$) lung sections. (*H*) Number of various airway epithelial cell types in P7 wild-type ($n = 5$) and *Shh-Ryk*^{cKO} ($n = 5$) lung sections. (*I*) Expression levels of airway epithelial cell markers in P7 wild-type ($n = 3$) and *Shh-Ryk*^{cKO} ($n = 3$) lungs by RT-qPCR. (*J*) WGA staining in wild-type ($n = 5$) and *CCSP-Ryk*^{cKO} ($n = 5$) lung sections at P7, P14, and P30. Error bars are means ± SEM; ns, not significant; $*P < 0.05$; $**P < 0.01$; $***P < 0.001$, 2-tailed Student's *t* test. Ct values are listed in *SI Appendix*, Table S2. (Scale bars: *A*, *F* [*Right*], *G*, and *J*, 30 μm; *C*, 1 mm; *D* and *E*, 100 μm; *F* [*Left*], 500 μm.)

in *Shh-Ryk*^{cKO} lungs compared to wild-type littermates (Fig. 4 *G* and *H*), the number of AGR2-positive goblet cells was increased, and that of club cells was significantly decreased (Fig. 4 *G* and *H*). In the airway epithelium of *Shh-Ryk*^{cKO} mice, basal (*SI Appendix*, Fig. S6*F*) and ciliated (*SI Appendix*, Fig. S6*G*) cell markers did not overlap with goblet cell markers; however, many goblet cells expressed club cell markers (*SI Appendix*, Fig. S6*G*), suggesting that the goblet cells derive from club cells and not from basal or ciliated cells. Additionally, while the proliferation of ciliated cells appeared to be unaltered, the number of proliferating goblet and club cells was significantly increased in *Shh-Ryk*^{cKO} lungs compared to wild-type littermates (*SI Appendix*, Fig. S6 *I* and *J*). To test the expression of airway epithelial cell markers in *Shh-Ryk*^{cKO} lungs, we performed RT-qPCR. Expression of the goblet cell genes *Foxa3*, *Agr2*, *Muc5ac*, and *Muc5b* was significantly up-regulated in *Shh-Ryk*^{cKO} lungs compared to wild type, while that of *Scgb1a1* was down-regulated (Fig. 4*I*). However, expression of *Foxj1*, *Krt5*, and *Spdef* did not appear to be significantly altered in *Shh-Ryk*^{cKO} lungs (Fig. 4*I*). Overall, these data indicate that RYK inhibits goblet cell differentiation in the airway epithelium.

Next, to delete *Ryk* in club cells, we crossed *CCSP-iCre-YFP* mice with *Ryk*^{flox} mice (hereafter *CCSP-Ryk*^{cKO}). RYK expression was reduced to undetectable levels in YFP-positive club cells compared to wild-type littermates (*SI Appendix*, Fig. S6*K*). As development progressed, the number of goblet cells gradually increased in the *CCSP-Ryk*^{cKO} airway epithelium compared to that in wild-type littermates (Fig. 4*J*), indicating that *Ryk* deficiency in club cells leads to goblet cell hyperplasia at postnatal stages. However, when *Ryk* was deleted in ciliated cells by using *Foxj1-CreER*^{T2}, we found no obvious lung phenotypes (*SI Appendix*, Fig. S7 *A*–*D*). Taken together, these data suggest that RYK has a cell-autonomous function in club cells to inhibit goblet cell differentiation and hyperplasia.

***Ryk* Deficiency Causes Goblet Cell Hyperplasia during Lung Regeneration.** As RYK is also strongly expressed in the lung epithelium at adult stages (*SI Appendix*, Fig. S4 *G* and *H*), we hypothesized that it might function during adult lung homeostasis and repair. To test this hypothesis, we first administered naphthalene to wild-type adult mice and collected lung samples at 0, 2, 7, 14, and 21 d postinjury (dpi). In mouse, club cells are more susceptible to naphthalene-induced airway injury than other epithelial cell types, and they are considered fully regenerated only at around 21 dpi (47, 48). We examined the expression of *Ryk*, *Muc5b*, and *Mycn* during wild-type lung repair. The expression of *Muc5b* was decreased at 2 and 5 dpi but reached peak expression at 14 dpi, after which time uninjured expression levels were restored at 21 dpi (Fig. 5*A*). In contrast, the expression of *Ryk* and *Mycn* gradually increased over time after injury (Fig. 5*A*). These data suggest that RYK is active upon airway epithelial cell injury.

To test whether *Ryk* haploinsufficiency can interfere with airway epithelial cell differentiation after injury, we administered naphthalene to wild-type and *Ryk*$^{SL/+}$ mice. At 21 dpi, wild-type lungs exhibited no significant differences in the epithelial cell populations compared to uninjured wild-type lungs (Fig. 5*B*). However, at 21 dpi, *Ryk*$^{SL/+}$ mice exhibited dramatically increased numbers of goblet cells and a reduced number of club cells, with no obvious differences in basal or ciliated cell populations (Fig. 5*B*), indicating that RYK is required for the maintenance of club cells after injury.

Furthermore, we tested whether *Ryk* deficiency in club cells led to defects in airway epithelial cell differentiation after injury by administering naphthalene to *CCSP-Ryk*^{cKO} mice. At 21 dpi,

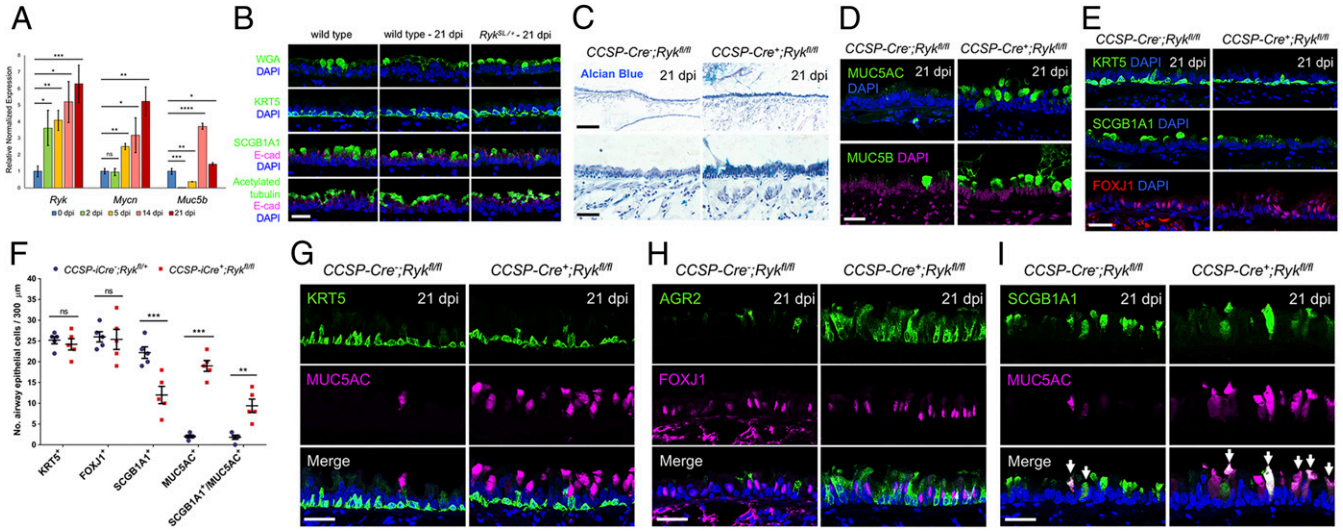

Fig. 5. Loss of *Ryk* function leads to goblet cell hyperplasia during lung regeneration. (*A*) Expression levels of *Ryk*, *Muc5b*, and *Mycn* during adult wild-type ($n = 3$) lung regeneration by RT-qPCR. (*B*) Immunostaining for airway epithelial cell markers in wild-type ($n = 5$) and $Ryk^{SL/+}$ ($n = 5$) lung sections during regeneration. (*C*) Alcian blue staining for mucus-secreting goblet cells in wild-type ($n = 6$) and *CCSP-Ryk*^{cKO} ($n = 6$) lung sections during regeneration. (*D*) Immunostaining for MUC5AC and MUC5B in wild-type ($n = 6$) and *CCSP-Ryk*^{cKO} ($n = 6$) lung sections during regeneration. (*E*) Immunostaining for airway epithelial cell markers in wild-type ($n = 6$) and *CCSP-Ryk*^{cKO} ($n = 6$) lung sections during regeneration. (*F*) Number of various airway epithelial cell types in wild-type ($n = 5$) and *CCSP-Ryk*^{cKO} ($n = 5$) lungs at 21 dpi. (*G*) Immunostaining for KRT5 and MUC5AC in wild-type ($n = 6$) and *CCSP-Ryk*^{cKO} ($n = 6$) lung sections during regeneration. (*H*) Immunostaining for AGR2 and FOXJ1 in wild-type ($n = 6$) and *CCSP-Ryk*^{cKO} ($n = 6$) lung sections during regeneration. (*I*) Immunostaining for SCGB1A1 and MUC5AC in wild-type ($n = 6$) and *CCSP-Ryk*^{cKO} ($n = 6$) lung sections during regeneration. Arrows point to overlapping expression between SCGB1A1 and MUC5AC. Error bars are means ± SEM; ns, not significant; $*P < 0.05$; $**P < 0.01$; $***P < 0.001$; $****P < 0.0001$, 2-tailed Student's *t* test. Ct values are listed in *SI Appendix*, Table S2. (Scale bars: *B*, *D*, *E*, and *G*–*I*, 30 μm; *C* [*Top*], 200 μm; *C* [*Bottom*], 50 μm.)

CCSP-Ryk^{cKO} mice exhibited mucus hypersecretion and increased numbers of goblet cells in the airway epithelium compared to wild-type littermates (Fig. 5*C*). The expression of MUC5AC and MUC5B and the number of goblet cells were dramatically increased in lungs with club cell-specific *Ryk* deletion compared to wild type (Fig. 5 *D* and *F*). At 21 dpi, while basal cells (KRT5$^+$) and ciliated cells (FOXJ1$^+$) were not changed in number, the number of club cells (SCGB1A1$^+$) was decreased in *CCSP-Ryk*^{cKO} airway epithelium (Fig. 5 *E* and *F*). In addition, during airway epithelial cell regeneration, basal cells and ciliated cells did not express MUC5AC and AGR2, respectively (Fig. 5 *G* and *H*). However, the expression of club cell markers, including CYP2F2, SCGB1A1, and SCGB3A1, was weakly detected in most goblet cells (AGR2$^+$ and MUC5AC$^+$) (Fig. 5*I* and *SI Appendix*, Fig. S7 *E* and *F*), suggesting that goblet cells may derive from club cells during airway epithelial cell regeneration. Moreover, in *CCSP-Ryk*^{cKO} lungs, NKX2-1 and SOX17 expression was not changed compared to wild type (*SI Appendix*, Fig. S5*G*), indicating that RYK does not participate in respiratory versus digestive fate determination during regeneration. Overall, these results suggest that RYK functions to maintain the balance among airway epithelial cell populations during lung regeneration.

Reduction of RYK Expression in COPD Patients' Airways. To determine whether RYK is expressed in human lungs, we examined control samples from embryonic and adult stages. Similar to our observations in mouse, RYK is specifically detected in the airway epithelium at early embryonic stages (Fig. 6*A*). At adult stages, RYK is strongly expressed in airway and alveolar epithelial cells (Fig. 6*B*), and weakly expressed in immune, endothelial, and smooth muscle cells (Fig. 6*C*).

Goblet cell metaplasia including hyperplasia is one of the characteristic features of asthma and COPD including emphysema and chronic bronchitis (1, 2). WNT/β-catenin signaling activity is decreased in COPD, and its reactivation can attenuate pathological features of COPD patient-derived cells and murine models (49, 50). In order to test whether RYK expression is altered in COPD patient lungs, we performed immunostaining. In samples from healthy donors, RYK was strongly detected in small airway epithelial cells and distal alveolar epithelial cells (Fig. 6*D* and *SI Appendix*, Fig. S8*A*). In contrast, while RYK was still strongly detected in alveolar epithelial cells, its expression in the airway epithelium was significantly reduced in samples from COPD patients exhibiting goblet cell metaplasia (Fig. 6*D* and *SI Appendix*, Fig. S8*A*). By immunostaining for RYK and MUC5AC in healthy donor and COPD patient samples, we observed reduced RYK expression in MUC5AC-positive cells (Fig. 6*E* and *SI Appendix*, Fig. S8*B*), indicating that RYK deficiency may lead to goblet cell metaplasia in the airway of COPD patients. Taken together, these data indicate that RYK may play a protective role against goblet cell metaplasia in COPD.

Discussion

Here, by performing an ENU mutagenesis screen, we identified a mutation in the mouse *Ryk* gene and investigated its role during lung development and repair. Our Ryk^{SL} mutant mice exhibit goblet cell hyperplasia and mucus hypersecretion, as well as growth retardation and lung inflammation. *Ryk* expression in the lung is strongly detected in airway epithelial cells and alveoli. Consistent with this expression pattern, lung epithelial cell-specific *Ryk* deletion led to goblet cell hyperplasia and mucus hypersecretion. These and other data indicate that RYK is a negative regulator of goblet cell differentiation by positively regulating WNT/β-catenin signaling during lung homeostasis and repair.

The WNT signaling pathway plays pivotal roles in cell fate determination, cell migration, and polarity in development, and it also controls stem cell self-renewal and tissue homeostasis during repair (51). RYK is a pseudokinase which participates in β-catenin–dependent and β-catenin–independent signaling in a cell- and tissue-dependent manner (18, 19, 26–29). For example, RYK potentiates WNT/β-catenin signaling when mammalian cells are treated with the canonical ligands WNT1 and WNT3a

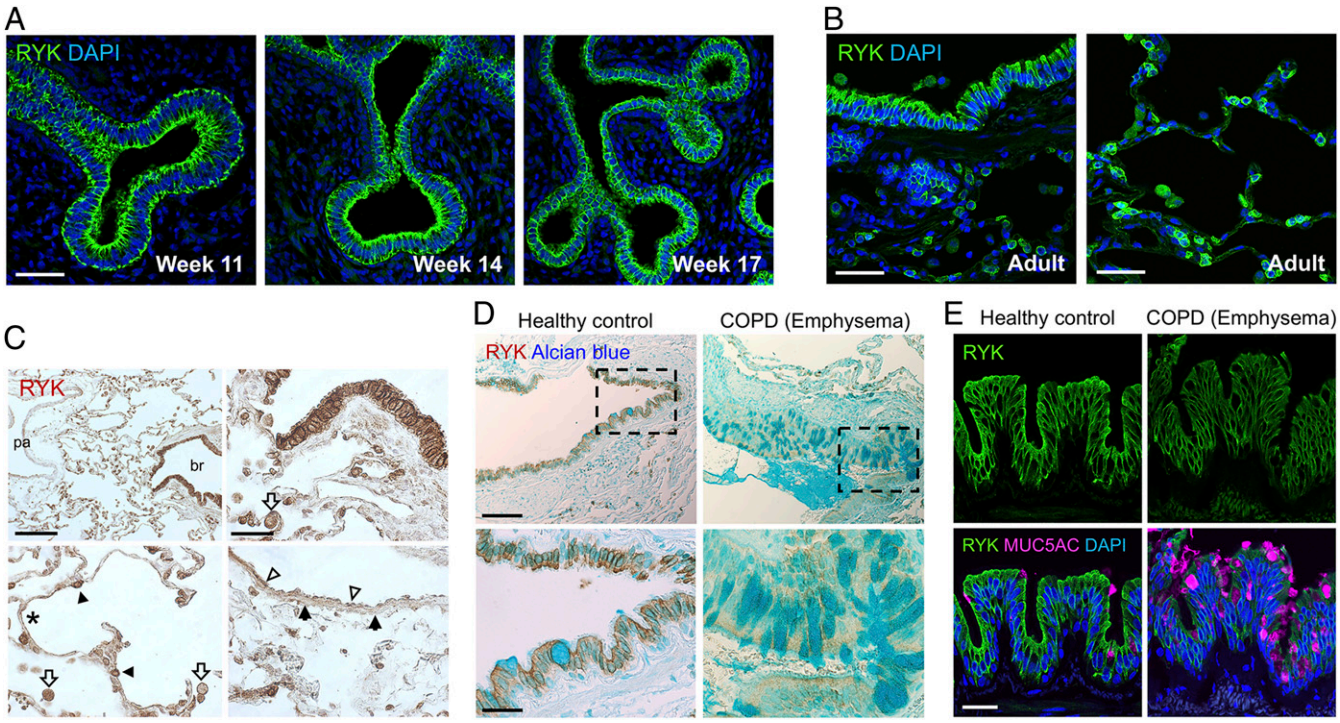

Fig. 6. Reduced RYK expression in COPD patients. (*A*) Immunostaining for RYK in human embryonic distal airway at week 11, 14, and 17. (*B*) Immunostaining for RYK in airway and alveoli of adult human lung sections. (*C*) Immunostaining for RYK in adult human lung sections. Open arrows, immune cells; asterisk, AT1 cell; arrowheads, AT2 cells; arrows, smooth muscle cells; open arrowheads, endothelial cells; br, bronchiole; pa, pulmonary artery. (*D*) Immunostaining for RYK and Alcian blue staining in lung sections from healthy donors and COPD patients. A high-magnification image of the area in the dashed boxes is shown on the *Bottom*. (*E*) Immunostaining for RYK and MUC5AC in lung sections from healthy donors and COPD patients. (Scale bars: *A*, *B* [*Right*], and *C* [*Right*], 50 μm; *B* [*Left*] and *D* [*Top*], 100 μm; *C* [*Left*], 200 μm; *D* [*Bottom*] and E, 30 μm.)

(26, 52). In zebrafish (21) and *Xenopus* (22), RYK can act as a receptor for Wnt5b and Wnt11, respectively, to activate PCP signaling. Similarly, in mammals, WNT5A/RYK regulates PCP signaling by stabilizing VANGL2, a core PCP pathway component (28). In the present study, using WNT reporters in vitro and in vivo, we found that RYK functions autonomously in the lung airway epithelium as a positive regulator of WNT/β-catenin signaling. RYK consists of a WNT-binding WIF domain at its N terminus, a transmembrane domain, a pseudokinase domain, and a PDZ-binding motif at its C terminus (18, 19). The SL mutation in the *Ryk* ENU allele leads to a 45-amino acid extension of its C terminus, preventing interaction with DVL and membrane localization (*SI Appendix*, Fig. S2 *D* and *E*). An SL mutation in mouse *cFlip* generates a peptide extension that interacts with an E3 ligase, leading to ubiquitination and proteasomal degradation (53), raising the possibility that the RYK^{SL} protein is highly unstable and thus subsequently degraded via the ubiquitin–proteasome system.

Airway epithelial cells represent the first line of defense against inhaled agents, including cigarette smoke, allergens, and microorganisms. Goblet cells secrete mucus as a physical barrier to protect the airway from dehydration, while trapping air particles which are swept away by mucociliary clearance (33). Under normal physiological conditions, the airway epithelium contains only a few goblet cells, and moderate secretion of mucus exerts a protective function. However, in response to acute or chronic airway injury, goblet cells undergo hyperplastic growth, followed by mucus hypersecretion, ultimately leading to mucous accumulation and airway obstruction, as well as infection (6, 7). Under these conditions, in vivo studies have shown that mouse club cells, but not ciliated cells, transdifferentiate into goblet cells (46, 54). These results are consistent with goblet cell hyperplasia originating from club cells in the *Ryk*-deficient epithelium, indicating that signaling through WNT/RYK, β-catenin, and MYCN plays an important role in the maintenance of club cell fate during lung development and repair. Goblet cell metaplasia is often observed in parallel with pulmonary inflammation, and inflammatory signals are proposed to drive the metaplastic transition (3, 6, 7). In contrast, *Ryk*-depleted airway epithelia exhibited goblet cell hyperplasia and mucus hypersecretion without inflammation, suggesting that inactivating mutations in *Ryk* are sufficient to drive goblet cell hyperplasia.

Acquisition of airway goblet cell fate is controlled by several signals, including inflammatory stimuli, growth factors, and transcription factors. Even though the ETS transcription factor SPDEF is a known master regulator of goblet cell differentiation and maturation (36, 37), SPDEF is not required for FOXA3-mediated goblet cell metaplasia (38), and its mRNA levels were not significantly altered in *Ryk* mutant lungs. In our in vitro and in vivo studies, loss of *Ryk* function caused increased expression of genes associated with goblet cell hyperplasia, including *Agr2*, *Muc5ac*, *Muc5b*, and *Foxa3*, but not *Spdef*. In addition, while SPDEF directly regulates *Muc5ac* expression, it does not affect *Muc5b* expression (55). In contrast, *Ryk* deficiency increased the expression of both *Muc5ac* and *Muc5b*, indicating that WNT/RYK signaling regulates mucin gene expression in the airway epithelium without affecting *Spdef* mRNA levels.

Goblet cell metaplasia/hyperplasia accompanied by mucus hypersecretion is a common feature of asthma, COPD, and pulmonary fibrosis (1, 2). In the lungs of COPD patients, WNT/β-catenin signaling has been reported to be down-regulated (56, 57), and smoking, a major risk factor in COPD, leads to reduced WNT/β-catenin activity in airway epithelia of COPD lungs. Moreover, activation of WNT/β-catenin signaling can attenuate pathological features of COPD patient-derived cells and murine models (49, 57, 58). By analyzing COPD/emphysema patient samples, we found that RYK expression was down-regulated in goblet cell metaplastic foci expressing MUC5AC and MUC5B in the small airways

(*SI Appendix*, Fig. S8 *B* and *C*). These data indicate that RYK has a protective role against goblet cell metaplasia in COPD lungs and warrant further studies on RYK as a diagnostic marker of disease progression, as it appears to correlate with goblet cell metaplasia and mucus hypersecretion. In COPD, reduced WNT/β-catenin signaling in the lung mesenchymal compartment results in lower cell proliferation rates, leading to mesenchymal deficiency, reduction of ECM protein expression in alveolar cells, and, as a consequence, emphysema and airway inflammation (50). Our results suggest that, in COPD patients, goblet cell metaplasia may be caused by defective epithelial cell proliferation or specification programs, rather than by inflammatory signals. In addition, we show that goblet cell fate is controlled by the WNT/RYK signaling pathway. Thus, we propose that therapeutic approaches for goblet cell metaplasia in COPD might exploit control of the WNT/β-catenin signaling pathway through RYK.

Materials and Methods

All animal care and experimental procedures in this study were approved by the local animal ethics committee at the Regierungspräsidium Darmstadt, Hessen, Germany. ENU-induced C57BL/6 males were obtained from Monica Justice, Baylor College of Medicine, Houston, TX. Tamoxifen (Sigma) was dissolved in corn oil (Sigma) at 50 mg/mL and injected intraperitoneally at the indicated developmental stages and frequencies. For whole-exome sequencing, genomic DNA samples were extracted from 2 wild types and 2 mutants. For RNA sequencing (RNA-Seq), total RNA was isolated from P1 lungs of 2 $Ryk^{+/+}$ and 2 $Ryk^{SL/SL}$ mice. Whole-exome sequencing and RNA-Seq were performed as previously described (39).

The materials and methods used in this study are described in detail in *SI Appendix, SI Materials and Methods*.

Data Availability. The RNA-Seq dataset produced in this study is available in the Gene Expression Omnibus (GEO) database, https://www.ncbi.nlm.nih.gov/geo/query/acc.cgi?acc=GSE131946 (accession no. GSE131946).

ACKNOWLEDGMENTS. We thank Saverio Bellusci for the *Shh-Cre* mice; Birgit Spiznagel, Isabelle Salwig, and Thomas Braun for the *CMV-Cre*, *CCSP-iCre-YFP*, and *Foxj1-CreER^{T2}* mice; and Srikanth Karnati for the C22 mouse club cell line. We also thank Young-June Jin, Felix Gunawan, Konstantinos Gkatzis, Josephine Gollin, and Simon Perathoner for discussions and/or critical reading of the manuscript. Y.N. was supported by grants-in-aid from the Japan Society for the Promotion of Science (Grant 19K22728). This work was supported by funds from the Max Planck Society to D.Y.R.S.

1. L. Cohn, Mucus in chronic airway diseases: Sorting out the sticky details. *J. Clin. Invest.* **116**, 306–308 (2006).
2. J. Ma, B. K. Rubin, J. A. Voynow, Mucins, mucus, and goblet cells. *Chest* **154**, 169–176 (2018).
3. D. R. Curran, L. Cohn, Advances in mucous cell metaplasia: A plug for mucus as a therapeutic focus in chronic airway disease. *Am. J. Respir. Cell Mol. Biol.* **42**, 268–275 (2010).
4. K. A. Schilders *et al.*, Regeneration of the lung: Lung stem cells and the development of lung mimicking devices. *Respir. Res.* **17**, 44 (2016).
5. A. T. Reid *et al.*, Persistent induction of goblet cell differentiation in the airways: Therapeutic approaches. *Pharmacol. Ther.* **185**, 155–169 (2018).
6. P. Thai, A. Loukoianov, S. Wachi, R. Wu, Regulation of airway mucin gene expression. *Annu. Rev. Physiol.* **70**, 405–429 (2008).
7. O. Boucherat, J. Boczkowski, L. Jeannotte, C. Delacourt, Cellular and molecular mechanisms of goblet cell metaplasia in the respiratory airways. *Exp. Lung Res.* **39**, 207–216 (2013).
8. C. Li, S. Bellusci, Z. Borok, P. Minoo, Non-canonical WNT signalling in the lung. *J. Biochem.* **158**, 355–365 (2015).
9. H. A. Baarsma, M. Königshoff, *'WNT-er is coming'*: WNT signalling in chronic lung diseases. *Thorax* **72**, 746–759 (2017).
10. M. Hussain *et al.*, Wnt/β-catenin signaling links embryonic lung development and asthmatic airway remodeling. *Biochim Biophys Acta Mol Basis Dis* **1863**, 3226–3242 (2017).
11. M. Zhang, J. Shi, Y. Huang, L. Lai, Expression of canonical WNT/β-CATENIN signaling components in the developing human lung. *BMC Dev. Biol.* **12**, 21 (2012).
12. A. M. Goss *et al.*, Wnt2/2b and β-catenin signaling are necessary and sufficient to specify lung progenitors in the foregut. *Dev. Cell* **17**, 290–298 (2009).
13. A. Caprioli *et al.*, Wnt4 is essential to normal mammalian lung development. *Dev. Biol.* **406**, 222–234 (2015).
14. C. Li, J. Xiao, K. Hormi, Z. Borok, P. Minoo, Wnt5a participates in distal lung morphogenesis. *Dev. Biol.* **248**, 68–81 (2002).
15. K. S. Harris-Johnson, E. T. Domyan, C. M. Vezina, X. Sun, β-Catenin promotes respiratory progenitor identity in mouse foregut. *Proc. Natl. Acad. Sci. U.S.A.* **106**, 16287–16292 (2009).
16. C. Li *et al.*, Stabilized β-catenin in lung epithelial cells changes cell fate and leads to tracheal and bronchial polyposis. *Dev. Biol.* **334**, 97–108 (2009).
17. M. L. Mucenski *et al.*, β-catenin regulates differentiation of respiratory epithelial cells in vivo. *Am. J. Physiol. Lung Cell. Mol. Physiol.* **289**, L971–L979 (2005).
18. J. Green, R. Nusse, R. van Amerongen, The role of Ryk and Ror receptor tyrosine kinases in Wnt signal transduction. *Cold Spring Harb. Perspect. Biol.* **6**, a009175 (2014).
19. M. M. Halford, M. L. Macheda, S. A. Stacker, "The RYK receptor family" in *Receptor Tyrosine Kinases: Family and Subfamilies*, D. L. Wheeler, Y. Yarden, Eds. (Humana, 2015), pp. 685–741.
20. J. L. Bonkowsky, S. Yoshikawa, D. D. O'Keefe, A. L. Scully, J. B. Thomas, Axon routing across the midline controlled by the *Drosophila* Derailed receptor. *Nature* **402**, 540–544 (1999).
21. S. Lin, L. M. Baye, T. A. Westfall, D. C. Slusarski, Wnt5b-Ryk pathway provides directional signals to regulate gastrulation movement. *J. Cell Biol.* **190**, 263–278 (2010).
22. G. H. Kim, J. H. Her, J. K. Han, Ryk cooperates with Frizzled 7 to promote Wnt11-mediated endocytosis and is essential for *Xenopus laevis* convergent extension movements. *J. Cell Biol.* **182**, 1073–1082 (2008).
23. M. M. Halford *et al.*, Ryk-deficient mice exhibit craniofacial defects associated with perturbed Eph receptor crosstalk. *Nat. Genet.* **25**, 414–418 (2000).
24. L. G. Fradkin, J. M. Dura, J. N. Noordermeer, Ryks: New partners for Wnts in the developing and regenerating nervous system. *Trends Neurosci.* **33**, 84–92 (2010).
25. J. P. Roy, M. M. Halford, S. A. Stacker, The biochemistry, signalling and disease relevance of RYK and other WNT-binding receptor tyrosine kinases. *Growth Factors* **36**, 15–40 (2018).
26. W. Lu, V. Yamamoto, B. Ortega, D. Baltimore, Mammalian Ryk is a Wnt coreceptor required for stimulation of neurite outgrowth. *Cell* **119**, 97–108 (2004).
27. A. M. Schmitt *et al.*, Wnt-Ryk signalling mediates medial-lateral retinotectal topographic mapping. *Nature* **439**, 31–37 (2006).
28. P. Andre *et al.*, The Wnt coreceptor Ryk regulates Wnt/planar cell polarity by modulating the degradation of the core planar cell polarity component Vangl2. *J. Biol. Chem.* **287**, 44518–44525 (2012).
29. M. L. Macheda *et al.*, The Wnt receptor Ryk plays a role in mammalian planar cell polarity signaling. *J. Biol. Chem.* **287**, 29312–29323 (2012).
30. K. Kessenbrock *et al.*, Diverse regulation of mammary epithelial growth and branching morphogenesis through noncanonical Wnt signaling. *Proc. Natl. Acad. Sci. U.S.A.* **114**, 3121–3126 (2017).
31. K. Kugathasan *et al.*, Deficiency of the Wnt receptor Ryk causes multiple cardiac and outflow tract defects. *Growth Factors* **36**, 58–68 (2018).
32. J. R. Rock, B. L. Hogan, Epithelial progenitor cells in lung development, maintenance, repair, and disease. *Annu. Rev. Cell Dev. Biol.* **27**, 493–512 (2011).
33. H. A. McCauley, G. Guasch, Three cheers for the goblet cell: Maintaining homeostasis in mucosal epithelia. *Trends Mol. Med.* **21**, 492–503 (2015).
34. J. S. Guseh *et al.*, Notch signaling promotes airway mucous metaplasia and inhibits alveolar development. *Development* **136**, 1751–1759 (2009).
35. S. Li *et al.*, Foxp1/4 control epithelial cell fate during lung development and regeneration through regulation of anterior gradient 2. *Development* **139**, 2500–2509 (2012).
36. K. S. Park *et al.*, SPDEF regulates goblet cell hyperplasia in the airway epithelium. *J. Clin. Invest.* **117**, 978–988 (2007).
37. P. Rajavelu *et al.*, Airway epithelial SPDEF integrates goblet cell differentiation and pulmonary Th2 inflammation. *J. Clin. Invest.* **125**, 2021–2031 (2015).
38. G. Chen *et al.*, Foxa3 induces goblet cell metaplasia and inhibits innate antiviral immunity. *Am. J. Respir. Crit. Care Med.* **189**, 301–313 (2014).
39. H. T. Kim *et al.*, Myh10 deficiency leads to defective extracellular matrix remodeling and pulmonary disease. *Nat. Commun.* **9**, 4600 (2018).
40. W. Yin *et al.*, The potassium channel KCNJ13 is essential for smooth muscle cytoskeletal organization during mouse tracheal tubulogenesis. *Nat. Commun.* **9**, 2815 (2018).
41. L. S. Ostedgaard *et al.*, Gel-forming mucins form distinct morphologic structures in airways. *Proc. Natl. Acad. Sci. U.S.A.* **114**, 6842–6847 (2017).
42. T. Okubo, P. S. Knoepfler, R. N. Eisenman, B. L. Hogan, Nmyc plays an essential role during lung development as a dosage-sensitive regulator of progenitor cell proliferation and differentiation. *Development* **132**, 1363–1374 (2005).
43. D. ten Berge, S. A. Brugmann, J. A. Helms, R. Nusse, Wnt and FGF signals interact to coordinate growth with cell fate specification during limb development. *Development* **135**, 3247–3257 (2008).
44. P. R. Tata *et al.*, Developmental history provides a roadmap for the emergence of tumor plasticity. *Dev. Cell* **44**, 679–693.e5 (2018).
45. C. W. Davis, B. F. Dickey, Regulated airway goblet cell mucin secretion. *Annu. Rev. Physiol.* **70**, 487–512 (2008).
46. C. M. Evans *et al.*, Mucin is produced by Clara cells in the proximal airways of antigen-challenged mice. *Am. J. Respir. Cell Mol. Biol.* **31**, 382–394 (2004).
47. C. G. Plopper, J. Macklin, S. J. Nishio, D. M. Hyde, A. R. Buckpitt, Relationship of cytochrome P-450 activity to Clara cell cytotoxicity. III. Morphometric comparison of changes in the epithelial populations of terminal bronchioles and lobar bronchi in mice, hamsters, and rats after parenteral administration of naphthalene. *Lab. Invest.* **67**, 553–565 (1992).

48. H. S. Hsu *et al*., Repair of naphthalene-induced acute tracheal injury by basal cells depends on β-catenin. *J. Thorac. Cardiovasc. Surg.* **148**, 322–332 (2014).
49. N. Kneidinger *et al*., Activation of the WNT/β-catenin pathway attenuates experimental emphysema. *Am. J. Respir. Crit. Care Med.* **183**, 723–733 (2011).
50. J. Shi, F. Li, M. Luo, J. Wei, X. Liu, Distinct roles of Wnt/β-catenin signaling in the pathogenesis of chronic obstructive pulmonary disease and idiopathic pulmonary fibrosis. *Mediators Inflamm.* **2017**, 3520581 (2017).
51. Z. Steinhart, S. Angers, Wnt signaling in development and tissue homeostasis. *Development* **145**, dev146589 (2018).
52. J. D. Berndt *et al*., Mindbomb 1, an E3 ubiquitin ligase, forms a complex with RYK to activate Wnt/β-catenin signaling. *J. Cell Biol.* **194**, 737–750 (2011).
53. N. Shibata *et al*., Degradation of stop codon read-through mutant proteins via the ubiquitin-proteasome system causes hereditary disorders. *J. Biol. Chem.* **290**, 28428–28437 (2015).
54. A. Pardo-Saganta, B. M. Law, M. Gonzalez-Celeiro, V. Vinarsky, J. Rajagopal, Ciliated cells of pseudostratified airway epithelium do not become mucous cells after ovalbumin challenge. *Am. J. Respir. Cell Mol. Biol.* **48**, 364–373 (2013).
55. G. Chen *et al*., Role of Spdef in the regulation of Muc5b expression in the airways of naive and mucoobstructed mice. *Am. J. Respir. Cell Mol. Biol.* **59**, 383–396 (2018).
56. R. Wang *et al*., Down-regulation of the canonical Wnt β-catenin pathway in the airway epithelium of healthy smokers and smokers with COPD. *PLoS One* **6**, e14793 (2011).
57. L. Guo *et al*., WNT/β-catenin signaling regulates cigarette smoke-induced airway inflammation via the PPARδ/p38 pathway. *Lab. Invest.* **96**, 218–229 (2016).
58. F. E. Uhl *et al*., Preclinical validation and imaging of Wnt-induced repair in human 3D lung tissue cultures. *Eur. Respir. J.* **46**, 1150–1166 (2015).